Chinese Journal of Aeronautics, (2020), xxx(xx): xxx–xxx

Chinese Society of Aeronautics and Astronautics
& Beihang University

Chinese Journal of Aeronautics

cja@buaa.edu.cn
www.sciencedirect.com

Formation flight of fixed-wing UAV swarms: A group-based hierarchical approach

Hao CHEN, Xiangke WANG *, Lincheng SHEN, Yirui CONG

College of Intelligence Science and Technology, National University of Defense Technology, Changsha 410073, China

Received 5 December 2019; revised 16 January 2020; accepted 6 March 2020

KEYWORDS

Control input constraints;
Coordinated path following;
Formation control;
Leader-following control;
Unmanned aerial vehicles swarms

Abstract This paper investigates a formation control problem of fixed-wing Unmanned Aerial Vehicle (UAV) swarms. A group-based hierarchical architecture is established among the UAVs, which decomposes all the UAVs into several distinct and non-overlapping groups. In each group, the UAVs form hierarchies with one UAV selected as the group leader. All group leaders execute coordinated path following to cooperatively handle the mission process among different groups, and the remaining followers track their direct leaders to achieve the inner-group coordination. More specifically, for a group leader, a virtual target moving along its desired path is assigned for the UAV, and an updating law is proposed to coordinate all the group leaders' virtual targets; for a follower UAV, the distributed leader-following formation control law is proposed to make the follower's heading angle coincide with its direct leader, while keeping the desired relative position with respect to its direct leader. The proposed control law guarantees the globally asymptotic stability of the whole closed-loop swarm system under the control input constraints of fixed-wing UAVs. Theoretical proofs and numerical simulations are provided, which corroborate the effectiveness of the proposed method.

1. Introduction

1.1. Motivation

Autonomous Unmanned Aerial Vehicle (UAV) swarms have emerged as a disruptive technology for their enhanced flexibility and robustness compared to a single vehicle.[1–4] In this paper, we target at the formation flight of fixed-wing UAV swarms, which have broad application prospects due to the long range and endurance of these platforms.[5–7] Although significant achievements have been reported in recent years (see Section 1.2), much work remains to be done to bridge the technological gaps and make the system applicable in more civil and military scenarios. The motivation of this paper stems from the following three aspects:

(1) In real applications, a swarm of UAVs are expected to accomplish complicated missions, which usually can be divided into several parallel subtasks, e.g., the multi-target search or tracking scenario.[8,9] In these cases, the UAVs need to be decomposed into several distinct and non-overlapping clusters/groups, with each cluster/

* Corresponding author.
E-mail address: xkwang@nudt.edu.cn (X. WANG).
Peer review under responsibility of Editorial Committee of CJA.

ELSEVIER Production and hosting by Elsevier

https://doi.org/10.1016/j.cja.2020.03.006

Please cite this article in press as: CHEN H et al. Formation flight of fixed-wing UAV swarms: A group-based hierarchical approach, *Chin J Aeronaut* (2020), https://doi.org/10.1016/j.cja.2020.03.006

group carrying out one subtask, while different clusters/groups are also required to coordinate as a whole. Although there has been extensive research on coordinated control, most of the existing results only focus on the coordination within one cluster/group.

(2) Currently, a common approach to achieve actual formation flight of UAV swarms is to pre-plan a path or a trajectory for each UAV in the swarm,[5,10,11] which calls for coordinated planning. Coordinated planning produces paths/trajectories avoiding obstacles and inter-UAV collision, while optimizing the mobility of the UAV swarm, minimizing the energy consumption, etc.[3] Coordinated planning involves a number of parameters, and when the number of UAVs grows up, it would be a challenging task to produce so many paths or trajectories within limited amount of time.[1,2]

(3) Fixed-wing UAVs are less maneuverable compared to their rotary-wing counterparts.[5,6,12] To be more precise, a fixed-wing UAV is constrained not only by the maximum forward speed and heading rate, but also by a minimum positive forward speed to support itself during the flight. These control input constraints bring additional challenges to the coordination of UAV swarms, since many traditional methods proposed in the reference, such as Ref.[13], cannot guarantee these constraints to be satisfied. If the control input constraints are not properly handled, the stability of the whole closed-loop swarm system would be influenced.

Therefore, it is necessary to develop efficient coordinated control methods satisfying the fixed-wing UAVs' control input constraints, and achieve coordination not only within the same group, but also among different groups in the swarm. In this paper, we focus on a group-based hierarchical approach to control fixed-wing UAV swarms, which can effectively handle the problems arising from the above three aspects.

1.2. Related work

Developing a swarm of UAVs has become a hot research topic in recent years. Nowadays, most of the UAV swarms reported are developed with rotary-wing drones. Industrial companies including Intel[1], EHang[2], High Great[3], etc., have performed light shows with swarms of more than one thousand UAVs. However, it is believed that these UAVs are programmed with predefined trajectories or centrally controlled.[10] In academic field, distributed formation control problem has been investigated by many researchers, and readers are referred to Refs.[14–16] for surveys of existing methods. Several typical approaches including displacement based control,[17] distance based control[18,19] and bearing based control,[20] etc, have been studied with rotary-wing UAV formations. In most of these works, all the UAVs coordinate in a single common group. In contrast, a swarm of twenty quadrotors were divided into several groups in Ref.[21], where the inter-group coordination is distributed, but the inner-group coordination is centralized.

Compared with rotary-wing UAVs, research on formation control of fixed-wing UAV swarms has received less attention. A vision-based leader-follower control method was proposed in Ref.[22] and validated by two UAVs, where a leader UAV is flying along the pre-planned path, and the follower UAV follows the leader by employing the onboard sensor measurements to obtain the relative states between two UAVs. Ref.[23] addressed the problem of driving multiple fixed-wing UAVs with non-identical constant forward speeds to reach stable circular motions, while their motion centers converge a particular formation shape. In Ref.[24], a novel approach, termed guidance-route based formation control method was proposed, which generates guidance commands for fixed-wing UAVs by designing guidance-route generation strategies. As a great advance in terms of the scale, live-fly of fifty fixed-wing UAVs was presented in Ref.[25]. Unfortunately, details of the control law were not provided in this work. We note that these works did not fully consider the fixed-wing UAVs' control input constraints, which is one of the main difficulties in controlling fixed-wing UAV swarms.[12,26,27] Since the fixed-wing UAVs are constrained by positive minimum positive forward speed, during the coordination process, a UAV cannot stop or become unacceptably slow to wait for another UAV. Besides, the heading rate and the forward speed are both with saturation constraints. Stability of the swarm needs to be investigated while meeting these constraints. In Ref.[28], a trajectory tracking control law was proposed, which satisfies a fixed-wing UAV's control input constraints. Based on this, a leader-follower formation control law was proposed in Ref.[29] for a group of followers to track a common leader.

Besides the above methods, another common way to achieve UAV formation flight is coordinated path following. Instead of tracking time-parameterized trajectories, the UAVs in the coordinated path following scenario follow geometric paths while trying to coordinate on some certain variables. Since a path need not be time-parameterized, it is more flexible to represent a path than to represent a trajectory. Several works in the literature discussed the coordinated path following control of fixed-wing UAVs. In Ref.[11], a coordinated path following control law was proposed to drive the UAVs to arrive at their respective destinations simultaneously. In Ref.[12], the UAVs are expected to maintain the desired along-path separations while following a common path. The coordinated moving path following problem was introduced in Ref.[27], where the desired path is moving on a plane. These works have considered some types of the control input constraints of fixed-wing UAVs. The minimum and maximum forward speed constraints were taken into account in all of these works, and the method in Ref.[12] even considered the heading rate constraints. However, in Ref.[12], only local stability is guaranteed for the closed-loop of the coordinated path following system, when all the constraints of fixed-wing UAVs are considered. A major requirement associated with coordinated path following is that each UAV needs to have access to a pre-planned path, which would be a challenging task to plan many paths for coordinated planning as the number of UAVs increases.

1.3. Contributions

The above related work motivates the research in this paper to deal with the formation flight of multiple groups of fixed-wing

[1] https://www.intel.com/content/www/us/en/technology-innovation/aerial-technology-light-show.html
[2] http://www.ehang.com/news/249.html
[3] http://droneshow.hg-fly.com/en/

Please cite this article in press as: CHEN H et al. Formation flight of fixed-wing UAV swarms: A group-based hierarchical approach, *Chin J Aeronaut* (2020), https://doi.org/10.1016/j.cja.2020.03.006

UAVs subject to control input constraints. The main contributions of this paper are summarized as follows:

(1) We propose a distributed and scalable group-based hierarchical control architecture for swarms of fixed-wing UAVs, and achieve both the inter-group coordination and inner-group coordination. With the proposed architecture, we do not need to plan paths for all the UAVs in the swarm, and thus reduce the complexity of coordinated planning.
(2) We propose the formation control law for leader UAVs and follower UAVs in each group, respectively. The proposed control law guarantees the globally asymptotic stability of the whole fixed-wing UAV swarm even with control input constraints. Numerical simulations demonstrate the effectiveness of the proposed method.

1.4. Paper organization

The remainder of this paper is organized as follows. Section 2 formulates the coordination problem of fixed-wing UAV swarms and presents the group-based hierarchical architecture. Section 3 proposes the distributed control law for the UAVs in the swarm. Simulations are presented in Section 4 to corroborate the theoretical results. Finally, concluding remarks are summarized in Section 5.

2. Problem formulation and architecture design

In this section, we formulate the problem of formation flight of fixed-wing UAV swarms, present our group-based hierarchical architecture, and obtain the error dynamics of the system. The UAVs employed in this paper are all homogeneous.

2.1. Problem statement

To fulfill a complicated mission, the fixed-wing UAVs sometimes need to be decomposed into several distinct and non-overlapping clusters, with each cluster executing a subtask. Besides, different clusters can merge into a common cluster according to the mission specification. Thus, the UAV swarms can form time-varying formation patterns during the flight.[30] As shown in the example in Fig. 1, in Stage I, the whole swarm are divided into two clusters, with each cluster patrolling in a designated area; and in Stage II, these two clusters merge into a common larger cluster to continue the mission process. To accomplish the whole mission, not only the UAVs in each cluster are required to reach a specific geometric formation pattern to carry out a subtask, but also the different clusters need to coordinate their schedule such that all the UAVs can merge into a common cluster at the desired place.

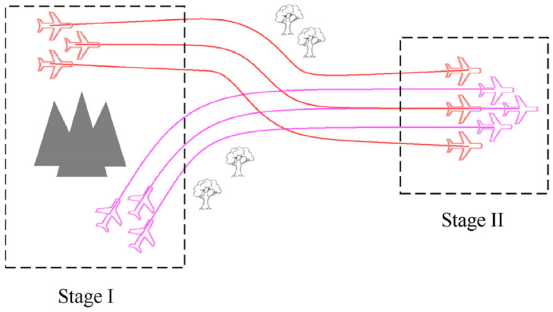

Fig. 1 Example of UAVs accomplishing a mission in several distinct and non-overlapping groups.

In many scenarios, the UAVs are flying at a constant altitude,[27,31,32] and we suppose each UAV has an independent altitude hold controller in its autopilot to hold the altitude constant. In that case, similar to Refs.[12,32], the movement of a fixed-wing UAV on 2D plane can be represented as:

$$\begin{cases} \dot{x}_i = v_i \cos\psi_i \\ \dot{y}_i = v_i \sin\psi_i \\ \dot{\psi}_i = \omega_i \end{cases} \tag{1}$$

where the subscript i is to denote the ith UAV, $[x_i, y_i]^{\mathrm{T}} \in \mathbf{R}^2$ is the UAV's center of mass in the inertial frame I, $\psi_i \in [-\pi, \pi)$ is the heading angle of the UAV with respect to the x axis of I, $[v_i, \omega_i]^{\mathrm{T}} \in \mathbf{R}^2$ are the control inputs of the kinematic fixed-wing UAV model, representing the forward speed and the heading rate of the UAV. It is noted that the fixed-wing UAVs are constrained by the following physical control input constraints:

$$0 < v_{\min} \leqslant v_i \leqslant v_{\max} \qquad -\omega_{\max} \leqslant \omega_i \leqslant \omega_{\max} \tag{2}$$

where $v_{\min}$ and $v_{\max}$ are the minimum and maximum forward speeds of the UAV, respectively, $\omega_{\max}$ is the maximum heading rate. For fixed-wing UAVs, the positive minimum forward speed $v_{\min}$ is necessary to guarantee sufficiently large lift to support the UAV during the flight, the maximum forward speed $v_{\max}$ results from the finite actuation power of the throttle, and the maximum heading rate $\omega_{\max}$ is caused by the boundedness of the roll angle to ensure safety of the UAV.

With the above formulations, the problem of coordinating fixed-wing UAV swarms can be formulated as follows:

Problem 1. Consider a swarm of fixed-wing UAVs in several clusters, and the kinematic model of each UAV is represented by Eq. (1) with constraints inequality (2). Design control scheme such that any two UAVs in the same cluster maintain the desired relative positions, and any two clusters in the swarm can merge into a common cluster when necessary.

2.2. Group-based hierarchical architecture

Hierarchical architecture provides an efficient tool to deal with complex systems.[33–35] In this architecture, all the UAVs are organized in several distinctive labeled groups, each group corresponds to a small cluster which will not be further decomposed during the mission execution process. By employing the group-based structure, we let the UAVs in the same group work together to complete the same subtask of a complicated mission. In each group, one UAV is selected as the group leader, and the other UAVs in the group are called followers as a whole. The UAVs in the same group form a tree topology with the group leader UAV as the root. Fig. 2 shows the group-based hierarchical architecture of n layers, consisting of one group leader layer, and n–1 follower layers. The group leaders communicate with each other to cooperatively handle the whole mission process, and they are also responsible for sending commands to their followers when necessary. The other

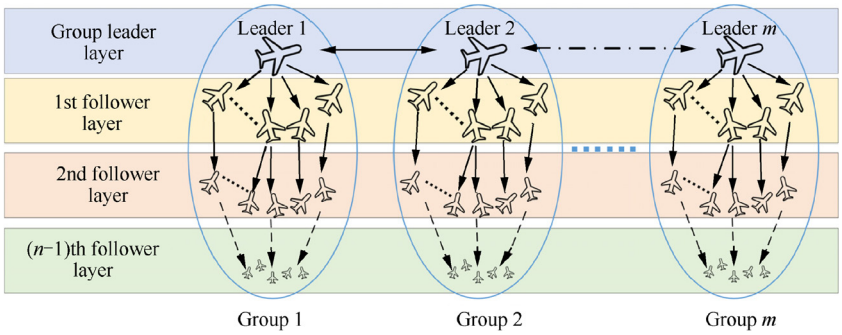

Fig. 2 Group-based hierarchical architecture of UAV swarms.

UAVs except the group leaders each has one neighbor, which can be regarded as this UAV's direct leader. The followers can obtain their direct leaders' states through communication or sensing, and they use their direct leaders' states and commands to coordinate with their direct leaders.

Based on the architecture shown in Fig. 2, when performing a mission, we first use coordinated planning methods to generate a series of paths for the group leaders to follow; then we design coordinated path following controllers to coordinate the group leaders, and distributed leader-following formation controllers to coordinate the other UAVs with respect to their direct leaders. Since the underlying network of the swarm is finite, if the UAVs in the group leader layer are coordinated, and the UAVs in the follower layers are coordinated with their direct leaders, then the whole swarm is well coordinated.

Before going on, we make some brief comments on the proposed architecture. Its main benefits can be summarized as follows:

(1) The proposed architecture is distributed, and we even do not need a global observer as in Ref.[36] to provide the global information of the UAV swarms. Therefore, it exploits parallelism and is suitable to handle large-scale swarms.
(2) Instead of making all the UAVs tightly coupled in an all-to-all communication network, the proposed architecture reduces the communication bandwidth, since only one UAV in each group, i.e., the group leader, needs to communicate with the UAVs in the other groups. Besides, the other UAVs except the group leaders only need the information from one UAV, i.e., the UAV's direct leader.
(3) In contrast to the approaches in Refs.[11,37] where all the UAVs need pre-planned paths to follow, the proposed architecture reduces the complexity of mission planning since the group leaders have the ability to guide the behaviors of the UAVs within the same group. As a result, we only need to plan paths for the group leaders. For the other UAVs, we can design distributed leader-following formation controllers to yield the desired formation patterns. Since the proposed architecture reduces the complexity of coordinated planning, it can be scaled to handle larger swarms of UAVs.
(4) In contrast to the leaderless self-organization process discussed in the swarm robotics community,[10,38] the proposed architecture provides guarantees on the formation pattern and rigidity of the structure. As a result, it would be easier to predict the motion of each UAV, and thus facilitate human operators monitoring the whole mission process.

Remark 1. It is assumed that the UAVs are equipped with onboard sensors to detect potential conflicts, and the cooperative conflict resolution approaches such as Ref. [31] can be employed when necessary. In this paper, we do not consider conflict resolution in the problem setup.

For notational convenience, we use $\mathcal{L}$ to denote the set of group leader UAVs, and $\mathcal{F}_i$ to denote the set of UAVs whose direct leader is the ith UAV.

2.3. Error dynamics

Based on the architecture in Section 2.2, the coordination of the whole swarm is twofold, i.e., the coordination of UAVs in the group leader layer, which corresponds to the inter-group coordination, and coordination of UAVs in the follower layers with respect to their direct leaders, which corresponds to the inner-group coordination. We discuss these two types of coordination one by one.

To coordinate the group leaders, we first use coordinated planning methods to generate a set of paths, and each group leader has a path to follow. Coordinated planning methods are out of the scope of this paper, and readers are referred to surveys in Refs.[39,40]. We assume that each path is globally known to the group leader that the path is assigned to. After generating the paths for the group leaders, we let these UAVs execute coordinated path following, instead of trajectory tracking as discussed in Ref.[28]. This consideration stems from two main reasons. Firstly, it is more convenient to represent a geometric path than to describe a time-parameterized trajectory. Secondly, the group leaders are most critical in the adopted architecture, and thus it calls for more robust strategies. Coordinated path following control is generally favored by researchers to yield this kind of robustness, since it is proven in Ref.[41] that trajectory tracking has fundamental performance limitations in the presence of unstable zero dynamics. Moreover, the performances of trajectory tracking are even worse in wind.[26,31]

In contrast to the coordinated path following problem in Ref.[12], where the control law is designed to drive the UAV towards its closest projection point on the path, in this paper, we assign a virtual target for each group leader on its corre-

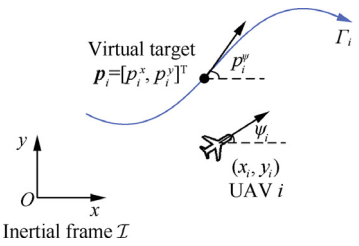

Fig. 3 Path following of a single group leader UAV i with its virtual target.

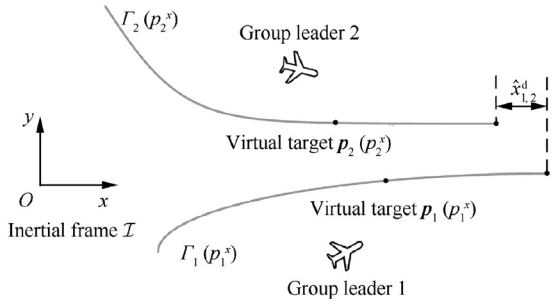

Fig. 4 An example to illustrate the coordinated path following of two group leader UAVs.

sponding path, and thus avoid the ambiguity when the closest projection point is not unique. Fig. 3 shows the path following of a single group leader UAV i as well as its virtual target on the path. The position of the virtual target in the inertial frame $\mathcal{I}$ is represented by $p_i = \left[p_i^x, p_i^y\right]^{\mathrm{T}}$, and the tangent direction of the path Γ_i at the virtual target point with respect to the x axis of $\mathcal{I}$ is represented by p_i^ψ. Thus the path following of a single group leader can be seen as steering the UAV towards its virtual target on the path, which means the control objective is $[x_i,y_i]^{\mathrm{T}} \to [p_i^x,p_i^y]^{\mathrm{T}}, \psi_i \to p_i^\psi, \forall i\, i \in \mathcal{L}$.

To achieve coordination of group leaders when they are following their respective paths, these UAVs' virtual targets on the paths should update in a coordinated manner. We use $\dot{s}_i$ to denote the progression rate of the ith UAV's virtual target, where s_i is the path-length parameter. We make the following assumption on each path Γ_i.

Assumption 1. For any $i \in \mathcal{L}$, Γ_i can be parameterized by a single variable θ_i, such that when θ_i is given, a point on the path can be uniquely determined. Besides, s_i is twice-differentiable with respect to θ_i, and $\frac{\mathrm{d}^2 s_i}{\mathrm{d}\theta_i^2}$ is bounded, $\frac{\mathrm{d}s_i}{\mathrm{d}\theta_i} \in [\alpha^-, \alpha^+], \kappa(\theta_i)\frac{\mathrm{d}s_i}{\mathrm{d}\theta_i} \in [-\beta^+, \beta^+]$, where $\alpha^-, \alpha^+, \beta^+ > 0$, $\kappa(\theta_i)$ is the signed curvature of the ith UAV's path at the point corresponding to θ_i.

Based on Assumption 1, p_i^x, p_i^y, p_i^ψ are all functions of θ_i. Therefore, we can use the value of θ_i to uniquely determine the virtual target point $\boldsymbol{p}_i$ of UAV i at time t. Moreover, it is further assumed that the parameterization of each path is conducted according to the mission specification, and the control objective of coordinating the group leaders' virtual targets is to achieve $\theta_i(t) - \theta_j(t) \to \theta_{ij}^{\mathrm{d}}$, where θ_{ij}^{d} is the desired difference between θ_i and θ_j. We use the following examples to provide further illustration.

Example 1. Fig. 4 shows an example where the paths of two group leaders are monotone in the direction of x axis. Thus the two paths can be parameterized as $\Gamma_i(p_i^x)$, and $\theta_i = p_i^x$ $(i = 1,2)$ in this example. Besides, these two group leaders are expected to have a desired separation $\hat{x}_{1,2}^{\mathrm{d}}$ along the x axis when following their respective paths. The control objective in this example is achieved if these two group leaders locate at their virtual target points, and $p_1^x - p_2^x \to \hat{x}_{1,2}^{\mathrm{d}}$.

We use an undirected network $\mathcal{G}_{\mathcal{L}} = (\mathcal{V}_{\mathcal{L}}, \mathcal{E}_{\mathcal{L}})$ to model the interaction among the group leaders, where $\mathcal{V}_{\mathcal{L}}$ is the set of vertices corresponding to the group leader set $\mathcal{L}$, and $\mathcal{E}_{\mathcal{L}}$ is the set of edges, with each edge modeling a peer-to-peer interaction among the group leaders. The ith group leader UAV's neighbor set $\mathcal{N}_i$ is the set of group leaders that are connected to i by an edge. Based on the above analysis, the coordinated path following control for the group leader UAVs can be described as follows:

Problem 2. Consider a set of $|\mathcal{L}|$ group leader UAVs modeled by Eqs. (1) and (2) under Assumption 1. Given an undirected network $\mathcal{G}_{\mathcal{L}} = (\mathcal{V}_{\mathcal{L}}, \mathcal{E}_{\mathcal{L}})$, find a control law for $i \in \mathcal{L}$ in the form of

$$\dot{s}_i = \sigma(\theta_i, \theta_j) \quad j \in \mathcal{N}_i \tag{3}$$

$$[v_i, \omega_i]^{\mathrm{T}} = \eta_1\left(\dot{s}_i, p_i^x, p_i^y, p_i^\psi, x_i, y_i, \psi_i\right) \tag{4}$$

where $\sigma(\cdot)$ and $\eta_1(\cdot)$ are functions, such that for any $i \in \mathcal{L}$, $j \in \mathcal{N}_i$,

$$\begin{cases} \lim\limits_{t\to\infty} x_i(t) - p_i^x(t) = 0, \\ \lim\limits_{t\to\infty} y_i(t) - p_i^y(t) = 0, \\ \lim\limits_{t\to\infty} \psi_i(t) - p_i^\psi(t) = 0, \\ \lim\limits_{t\to\infty} \theta_i(t) - \theta_j(t) = \theta_{ij}^{\mathrm{d}} \end{cases} \tag{5}$$

Remark 2. The variables θ_{ij}^{d} $(i,j \in \mathcal{L})$ should be properly selected to make the leader coordination mission valid. That is, for any θ_{ij}^{d} and $i,j \in \mathcal{L}$, there should exist $\theta_i^{\mathrm{d}}, \theta_j^{\mathrm{d}} \in \mathbf{R}$ such that $\theta_{ij}^{\mathrm{d}} = \theta_i^{\mathrm{d}} - \theta_j^{\mathrm{d}}$. A counterexample is $\theta_{1,2}^{\mathrm{d}} = 1, \theta_{2,3}^{\mathrm{d}} = 1, \theta_{1,3}^{\mathrm{d}} = -1$. In this case, one cannot find $\theta_1^{\mathrm{d}}, \theta_2^{\mathrm{d}}, \theta_3^{\mathrm{d}} \in \mathbf{R}$, such that $\theta_{1,2}^{\mathrm{d}} = \theta_1^{\mathrm{d}} - \theta_2^{\mathrm{d}}, \theta_{2,3}^{\mathrm{d}} = \theta_2^{\mathrm{d}} - \theta_3^{\mathrm{d}}$, and $\theta_{1,3}^{\mathrm{d}} = \theta_1^{\mathrm{d}} - \theta_3^{\mathrm{d}}$ all hold. Therefore, the selection of θ_{ij}^{d} should be in accordance with the celebrated Kirchhoff's voltage law; see Ref.[42] for more details.

Now we discuss the coordination control of follower UAVs with respect to their direct leaders, which is the inner-group coordination. Generally, in each cluster, the UAVs are required to maintain a geometric formation pattern during the formation flight.[8] Thus, the objective of controlling a follower UAV is to let its heading angle coincide with its direct leader, while keeping the desired relative position with respect to its direct leader. It is assumed that each follower knows its direct leader's states, including the position, heading angle, and the control inputs. Therefore, the follower control problem can be formulated as follows:

Problem 3. Find a control law for a follower UAV i ($i \in \mathcal{F}_l$) modeled by Eqs. (1) and (2) in the form of

$$[v_i, \omega_i]^{\mathrm{T}} = \eta_2(v_l, \omega_l, x_l, y_l, \psi_l, x_i, y_i, \psi_i) \tag{6}$$

where $\eta_2(\cdot)$ is a function, such that

$$\begin{cases} \lim\limits_{t\to\infty} x_i(t) - x_l(t) = d_i^x, \\ \lim\limits_{t\to\infty} y_i(t) - y_l(t) = d_i^y, \\ \lim\limits_{t\to\infty} \psi_i(t) - \psi_l(t) = 0 \end{cases} \tag{7}$$

where $[d_i^x, d_i^y]^{\mathrm{T}}$ is the desired relative position of follower i with respect to its direct leader l.

Remark 3. If Problem 2 is solved, it means the group leaders are well coordinated; and if Problem 3 is solved, it means the UAVs in each group are well coordinated. Therefore, with the group-based hierarchical architecture, if Problem 2 and Problem 3 are solved together, then Problem 1 is solved.

3. Control law design

In this section, we present the control law design in three steps. Firstly, a tracking control law considering the control input constraints of fixed-wing UAVs is presented, which will later be utilized by both the group leaders and the followers. Secondly, an updating law is proposed to coordinate the group leaders' virtual targets. Based on these results, we finally specify the control law for each type of UAVs.

3.1. Tracking control law design

By comparing Eqs. (4) and (6), it can be found that they are in a similar form: the group leaders are tracking their virtual targets, which are moving on their respective paths, and the followers are tracking their direct leaders. Therefore, we design a common tracking control law which can be employed by both types of UAVs, and the tracking problem is formulated as follows:

Problem 4. Consider vehicle 0 modeled by Eq. (1), with its position represented by $[x_0, y_0]^{\mathrm{T}}$, heading by ψ_0, forward speed by $v_0 \in [v_0^-, v_0^+] \subset [v_{\min}, v_{\max}]$, and heading rate by $\omega_0 \in [-\omega_0^+, \omega_0^+] \subset [-\omega_{\max}, \omega_{\max}]$, find a control law for UAV i modeled by Eqs. (1) and (2) in the form of

$$[v_i, \omega_i]^{\mathrm{T}} = \eta_0(v_0, \omega_0, x_i - x_0, y_i - y_0, \psi_i - \psi_0) \tag{8}$$

where $\eta_0(\cdot)$ is a function, such that

$$\begin{cases} \lim\limits_{t\to\infty} x_i(t) - x_0(t) = d_i^x, \\ \lim\limits_{t\to\infty} y_i(t) - y_0(t) = d_i^y, \\ \lim\limits_{t\to\infty} \psi_i(t) - \psi_0(t) = 0 \end{cases} \tag{9}$$

where $[d_i^x, d_i^y]^{\mathrm{T}}$ is the desired relative position of UAV i with respect to vehicle 0.

To solve Problem 4, we first represent the tracking errors in the ith UAV's body frame by using the following coordinate transformation, as shown in Fig. 5.

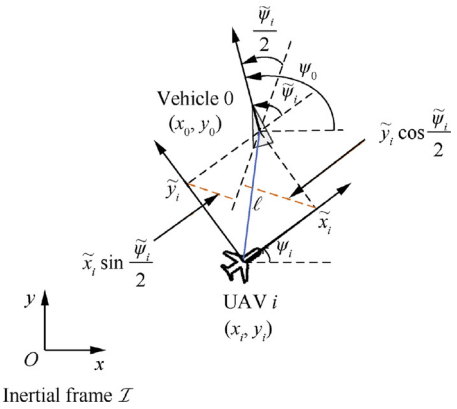

Fig. 5 Illustration of the tracking control.

$$\begin{bmatrix} \tilde{x}_i \\ \tilde{y}_i \\ \tilde{\psi}_i \end{bmatrix} = \begin{bmatrix} \cos\psi_i & \sin\psi_i & 0 \\ -\sin\psi_i & \cos\psi_i & 0 \\ 0 & 0 & 1 \end{bmatrix} \begin{bmatrix} x_0 - x_i + d_i^x \\ y_0 - y_i + d_i^y \\ \psi_0 - \psi_i \end{bmatrix} \tag{10}$$

Note that $\tilde{\psi}_i$ is an angle, and thus it can be made that $\tilde{\psi}_i \in [-\pi, \pi)$. To achieve the objective represented by Eq. (9), it suffices to show that for all initial states $[\tilde{x}_i(t_0), \tilde{y}_i(t_0)]^{\mathrm{T}} \in \mathbf{R}^2$ and $\tilde{\psi}_i(t_0) \in [-\pi, \pi)$,

$$\lim_{t\to\infty} \tilde{x}_i(t) = 0, \qquad \lim_{t\to\infty} \tilde{y}_i(t) = 0, \qquad \lim_{t\to\infty} \tilde{\psi}_i(t) = 0 \tag{11}$$

Eq. (10) together with Eq. (1) yields the following dynamics:

$$\begin{cases} \dot{\tilde{x}}_i = \omega_i \tilde{y}_i - v_i + v_0 \cos\tilde{\psi}_i \\ \dot{\tilde{y}}_i = -\omega_i \tilde{x}_i + v_0 \sin\tilde{\psi}_i \\ \dot{\tilde{\psi}}_i = \omega_0 - \omega_i \end{cases} \tag{12}$$

The tracking control law in the form of Eq. (18) is designed as follows:

$$v_i = v_0 + \frac{k_1 \tilde{x}_i}{\sqrt{\tilde{x}_i^2 + \tilde{y}_i^2 + \delta}} \tag{13}$$

$$\omega_i = \omega_0 + \frac{k_2 v_0 \left(-\tilde{x}_i \sin\frac{\tilde{\psi}_i}{2} + \tilde{y}_i \cos\frac{\tilde{\psi}_i}{2} \right)}{\sqrt{\tilde{x}_i^2 + \tilde{y}_i^2 + \delta}} + k_3 \sin\frac{\tilde{\psi}_i}{2} \tag{14}$$

where k_1,k_2,k_3 and δ are positive constants.

Remark 4. The second term in Eq. (13) is to reduce the absolute value of $\tilde{x}_i$, and the third term in Eq. (14) is to make $\tilde{\psi}_i$ converge to zero. Let ℓ be the line passing through the positions of UAV i and vehicle 0, as shown in Fig. 5, then the second term in Eq. is to drive the angle between the line ℓ and the heading of vehicle 0 towards $\frac{\tilde{\psi}_i}{2}$. Thus when this angle converges to $\frac{\tilde{\psi}_i}{2}$, and both $\tilde{x}_i$ and $\tilde{\psi}_i$ converge to zero, $\tilde{y}_i$ also converges to zero. In this way, the tracking control objective can be achieved, and the UAV's control inputs converge to v_0 and ω_0.

The following lemma states that the tracking problem can be solved by properly selecting parameters k_1, k_2, and k_3.

Lemma 1. Consider vehicle 0 with its movement satisfying Eq. (1), if $v_0 \in [v_0^-, v_0^+]$ and $\omega_0 \in [-\omega_0^+, \omega_0^+]$, where $[v_0^-, v_0^+] \subset [v_{\min}, v_{\max}], [-\omega_0^+, \omega_0^+] \subset [-\omega_{\max}, \omega_{\max}]$, $\dot{v}_0$ exists and is bounded, then by selecting parameters k_1, k_2 and k_3 such that Eq. (15) holds, control law Eqs. (13) and (14) can make variables $\tilde{x}_i, \tilde{y}_i, \dot{\tilde{x}}_i, \dot{\tilde{y}}_i, \dot{\tilde{\psi}}_i$ in Eq. (12) bounded, and solve Problem 4 for UAV i whose kinematic model satisfying Eqs. (1) and (2).

$$\begin{cases} k_1 \leqslant \min(v_{\max} - v_0^+, v_0^- - v_{\min}) \\ \omega_0^+ + k_2 v_0^+ + k_3 \leqslant \omega_{\max} \end{cases} \tag{15}$$

Proof. Firstly, note that $\left|\frac{\tilde{x}_i}{\sqrt{\tilde{x}_i^2+\tilde{y}_i^2+\delta}}\right| < 1, \left|\frac{-\tilde{x}_i\sin(\cdot)+\tilde{y}_i\cos(\cdot)}{\sqrt{\tilde{x}_i^2+\tilde{y}_i^2+\delta}}\right| < 1$, and $|\sin(\cdot)| < 1$. Therefore, it is obvious that if Eq. (15) holds, then Eq. (2) is satisfied.

Next, consider the following Lyapunov function candidate

$$V_1 = k_2\sqrt{\tilde{x}_i^2 + \tilde{y}_i^2 + \delta} + 8\sin^2\frac{\tilde{\psi}_i}{4} \tag{16}$$

We conclude $\lim_{t\to\infty}\tilde{x}_i(t) = 0, \lim_{t\to\infty}\tilde{y}_i(t) = 0, \lim_{t\to\infty}\tilde{\psi}_i(t) = 0$ by mimicking the proof of Theorem 1 in Ref.[28].

Control laws (13)–(14) can be employed by both types of UAVs in the swarm. When they are employed by a group leader, vehicle 0 in Problem 4 corresponds to the virtual target of this group leader, and $[d_i^x, d_i^y]^{\mathrm{T}} = [0, 0]^{\mathrm{T}}$; on the other hand, when control laws (13)–(14) are employed by a follower UAV, vehicle 0 is a real UAV platform, corresponding to the follower UAV's direct leader.

3.2. Updating law for group leaders' virtual targets

The tracking control law proposed in Section 3.1 can be employed by the group leaders to track their virtual targets on their paths. However, to achieve the coordinated path following control of group leader UAVs, an updating law to coordinate the leaders' virtual targets is needed. The aim is to achieve $\lim_{t\to\infty}\theta_i(t) - \theta_j(t) = \theta_{ij}^{\mathrm{d}}$ for any $i \in \mathcal{L}, j \in \mathcal{N}_i$. The updating law in the form of Eq. (3) is designed as:

$$\dot{\theta}_i = \mathrm{Sat}\left(\sum_{j\in\mathcal{N}_i} w_{ij}(\theta_j + \theta_{ij}^{\mathrm{d}} - \theta_i), -\gamma^+, \gamma^+\right) + \gamma_{\mathrm{d}} \tag{17}$$

$$\dot{s}_i = \frac{\mathrm{d}s_i}{\mathrm{d}\theta_i}\dot{\theta}_i \tag{18}$$

where $w_{ij} = w_{ji} > 0$, $\gamma_{\mathrm{d}}, \gamma^+ > 0$ and $\gamma_{\mathrm{d}} - \gamma^+ > 0$, the saturation function $z = \mathrm{Sat}(x, a, b) : \mathbf{R} \to \mathbf{R}$, where $a < b$ is defined as $z = a$ if $x < a$; $z = b$ if $x > b$; and $z = x$ otherwise. The following lemma states that the virtual targets of the group leaders can be coordinated with the updating laws (17)–(18).

Lemma 2. Consider a set of $|\mathcal{L}|$ group leader UAVs interacting through an undirected network $\mathcal{G}_{\mathcal{L}} = (\mathcal{V}_{\mathcal{L}}, \mathcal{E}_{\mathcal{L}})$. The proposed updating laws (17)–(18) for the group leaders' virtual targets guarantees $\lim_{t\to\infty}\theta_i(t) - \theta_j(t) = \theta_{ij}^{\mathrm{d}}$ for any $i \in \mathcal{L}, j \in \mathcal{N}_i$.

Proof. Define

$$u_i = \sum_{j\in\mathcal{N}_i} w_{ij}(\theta_j + \theta_{ij}^{\mathrm{d}} - \theta_i) \tag{19}$$

combining Eq. (17) with Eq. (19), we get

$$\dot{\theta}_i = \mathrm{Sat}(u_i, -\gamma^+, \gamma^+) + \gamma_{\mathrm{d}} \tag{20}$$

Consider the Lyapunov function candidate

$$V_2 = \frac{1}{2}\sum_{|\mathcal{L}|}\sum_{j\in\mathcal{N}_i} w_{ij}(\theta_i - \theta_j - \theta_{ij}^{\mathrm{d}})^2 \tag{21}$$

Differentiating Eq. (21) with respect to time, and using Eqs. (19) and (20), it yields,

$$\begin{aligned} \dot{V}_2 &= \sum_{|\mathcal{L}|}\sum_{j\in\mathcal{N}_i} w_{ij}(\theta_i - \theta_j - \theta_{ij}^{\mathrm{d}})(\dot{\theta}_i - \dot{\theta}_j) \\ &= -\sum_{|\mathcal{L}|} u_i \cdot \mathrm{Sat}(u_i, -\gamma^+, \gamma^+) - \sum_{|\mathcal{L}|}\sum_{j\in\mathcal{N}_i} w_{ij}(\theta_i - \theta_j \\ &\quad - \theta_{ij}^{\mathrm{d}}) \cdot \mathrm{Sat}(u_j, -\gamma^+, \gamma^+) \end{aligned} \tag{22}$$

Since $\mathcal{G}_{\mathcal{L}} = (\mathcal{V}_{\mathcal{L}}, \mathcal{E}_{\mathcal{L}})$ is an undirected network, and thus $j \in \mathcal{N}_i$ leads to $i \in \mathcal{N}_j$, and

$$\begin{aligned} &\sum_{|\mathcal{L}|}\sum_{j\in\mathcal{N}_i} w_{ij}(\theta_i - \theta_j - \theta_{ij}^{\mathrm{d}})\mathrm{Sat}(u_j, -\gamma^+, \gamma^+) \\ &= \sum_{|\mathcal{L}|}\sum_{j\in\mathcal{N}_i} w_{ji}(\theta_j - \theta_i + \theta_{ij}^{\mathrm{d}})\mathrm{Sat}(u_i, -\gamma^+, \gamma^+) \\ &= \sum_{|\mathcal{L}|}\sum_{j\in\mathcal{N}_i} w_{ij}(\theta_j - \theta_i + \theta_{ij}^{\mathrm{d}})\mathrm{Sat}(u_i, -\gamma^+, \gamma^+) \\ &= \sum_{|\mathcal{L}|} u_i\mathrm{Sat}(u_i, -\gamma^+, \gamma^+) \end{aligned} \tag{23}$$

Combining Eq. (22) with Eq. (23), we derive

$$\dot{V}_2 = -2\sum_{|\mathcal{L}|} u_i\mathrm{Sat}(u_i, -\gamma^+, \gamma^+) \leqslant 0 \tag{24}$$

and $\dot{V}_2 = 0$ if and only if $u_i = 0 (\forall i \in \mathcal{L})$. With Eq. (24), it can be deduced from the celebrated LaSalle's Invariance Principle[43] that $\lim_{t\to\infty} u_i = 0$ $(i \in \mathcal{L})$. Recall Remark 2 that $\theta_{ij}^{\mathrm{d}} = \theta_i^{\mathrm{d}} - \theta_j^{\mathrm{d}}$. Denote $u = \mathrm{col}(u_1, u_2, \ldots, u_{|\mathcal{L}|})$, $\theta = \mathrm{col}(\theta_1, \theta_2, \ldots, \theta_{|\mathcal{L}|})$, $\theta^{\mathrm{d}} = \mathrm{col}(\theta_1^{\mathrm{d}}, \theta_2^{\mathrm{d}}, \ldots, \theta_{|\mathcal{L}|}^{\mathrm{d}})$. Thus we can write Eq. (19) as

$$u = -L_{\mathrm{g}}(\mathcal{G}_{\mathcal{L}})(\theta - \theta^{\mathrm{d}}) \tag{25}$$

where $L_{\mathrm{g}}(\mathcal{G}_{\mathcal{L}})$ is the weighted Laplacian matrix[44] of the underlying graph $\mathcal{G}_{\mathcal{L}} = (\mathcal{V}_{\mathcal{L}}, \mathcal{E}_{\mathcal{L}})$. Note that the dimension of the null space of $L_{\mathrm{g}}(\mathcal{G}_{\mathcal{L}})$ equals the number of connected components in $\mathcal{G}_{\mathcal{L}}$, and $\lim_{t\to\infty} u(t) = 0$ leads to $\lim_{t\to\infty}\theta_i(t) - \theta_i^{\mathrm{d}} = \lim_{t\to\infty}\theta_j(t) - \theta_j^{\mathrm{d}}$ for i, j in the same connected component.[44] Thus $\lim_{t\to\infty}\theta_i(t) - \theta_j(t) = \theta_{ij}^{\mathrm{d}}$ holds for all $i \in \mathcal{L}$, $j \in \mathcal{N}_i$. □

Please cite this article in press as: CHEN H et al. Formation flight of fixed-wing UAV swarms: A group-based hierarchical approach, *Chin J Aeronaut* (2020), https://doi.org/10.1016/j.cja.2020.03.006

3.3. Control law for each type of UAVs

With the above results in Sections 3.1 and 3.2, we are now able to specify the control law for each type of UAVs.

For group leaders, they are tracking the virtual targets that are moving on their respective paths. The movement of a virtual target follows the updating law (17)-(18). Based on the tracking control law (13)-(14), the control law for $i \in \mathcal{L}$ in the form of Eq. (4) is designed as:

$$v_i = \dot{s}_i + \frac{k_1^{\mathrm{g}} \tilde{x}_i}{\sqrt{\tilde{x}_i^2 + \tilde{y}_i^2 + \delta}} \tag{26}$$

$$\omega_i = \kappa(\theta_i)\dot{s}_i + \frac{k_2^{\mathrm{g}} \dot{s}_i \left(-\tilde{x}_i \sin\frac{\tilde{\psi}_i}{2} + \tilde{y}_i \cos\frac{\tilde{\psi}_i}{2}\right)}{\sqrt{\tilde{x}_i^2 + \tilde{y}_i^2 + \delta}} + k_3^{\mathrm{g}} \sin\frac{\tilde{\psi}_i}{2} \tag{27}$$

where k_1^{g}, k_2^{g} and k_3^{g} are positive constants. Similar to Eq. (15), they satisfy

$$\begin{aligned} k_1^{\mathrm{g}} \leqslant & \min(v_{\mathrm{g}}^+ - \alpha^+(\gamma_{\mathrm{d}} + \gamma^+), \alpha^-(\gamma_{\mathrm{d}} - \gamma^+) - v_{\mathrm{g}}^-)\beta^+(\gamma_{\mathrm{d}} + \gamma^+) \\ & + k_2^{\mathrm{g}} \alpha^+(\gamma_{\mathrm{d}} + \gamma^+) + k_3^{\mathrm{g}} \leqslant \omega_{\mathrm{g}}^+ \end{aligned} \tag{28}$$

with $v_{\min} < v_{\mathrm{d}}^- < v_{\mathrm{d}}^+ < v_{\max}$, $\omega_{\mathrm{g}}^+ < \omega_{\max}$, and $\tilde{x}_i$, $\tilde{y}_i$, $\tilde{\psi}_i$ in Eqs. (26) and (27) are defined in a similar way to Eq. (10) as follows:

$$\begin{bmatrix} \tilde{x}_i \\ \tilde{y}_i \\ \tilde{\psi}_i \end{bmatrix} = \begin{bmatrix} \cos\psi_i & \sin\psi_i & 0 \\ -\sin\psi_i & \cos\psi_i & 0 \\ 0 & 0 & 1 \end{bmatrix} \begin{bmatrix} p_i^x - x_i \\ p_i^y - y_i \\ p_i^\psi - \psi_i \end{bmatrix} \tag{29}$$

The following theorem indicates the stability of the group leader control closed-loop.

Theorem 1. Group leader control stability. Consider a set of $|\mathcal{L}|$ group leader UAVs interacting through an undirected network $\mathcal{G}_{\mathcal{L}} = (\mathcal{V}_{\mathcal{L}}, \mathcal{E}_{\mathcal{L}})$, and Assumption 1 holds. If inequalities in Eq. hold, then Problem 2 can be solved by the control laws (17)–(18) and Eqs. (26) and (27). Moreover, variables $\tilde{x}_i$, $\tilde{y}_i$, $\dot{\tilde{x}}_i$, $\dot{\tilde{y}}_i$, $\dot{\tilde{\psi}}_i$ are all bounded, and each group leader's control inputs satisfy $v_i \in [v_{\mathrm{g}}^-, v_{\mathrm{g}}^+]$, $\omega_i \in [-\omega_{\mathrm{g}}^+, \omega_{\mathrm{g}}^+]$ $(i \in \mathcal{L})$.

Proof. It follows from Eqs. (17) and (18) and Assumption 1 that

$$\begin{cases} \dot{s}_i \in [\alpha^-(\gamma_{\mathrm{d}} - \gamma^+), \alpha^+(\gamma_{\mathrm{d}} + \gamma^+)] \\ \kappa(\theta_i)\dot{s}_i \in [-\beta^+(\gamma_{\mathrm{d}} + \gamma^+), \beta^+(\gamma_{\mathrm{d}} + \gamma^+)] \end{cases} \tag{30}$$

Combining Eqs. (26)–(28) with inequality (30), it yields $v_i \in [v_{\mathrm{g}}^-, v_{\mathrm{g}}^+]$, $\omega_i \in [-\omega_{\mathrm{g}}^+, \omega_{\mathrm{g}}^+]$. Note that $\ddot{s}_i$ exists and is bounded under Assumption 1 and the updating law (17)–(18), then it follows from Lemma 1 that $\lim_{t\to\infty} \tilde{x}_i(t) = 0$, $\lim_{t\to\infty} \tilde{y}_i(t) = 0$, $\lim_{t\to\infty} \tilde{\psi}_i(t) = 0$. By using Eq. (29), we obtain $\lim_{t\to\infty} p_i^x(t) - x_i(t) = 0$, $\lim_{t\to\infty} p_i^y(t) - y_i(t) = 0$, $\lim_{t\to\infty} p_i^\psi(t) - \psi_i(t) = 0$, and the variables $\tilde{x}_i$, $\tilde{y}_i$, $\dot{\tilde{x}}_i$, $\dot{\tilde{y}}_i$, $\dot{\tilde{\psi}}_i$ are all bounded. Besides, it follows from Lemma 2 that $\lim_{t\to\infty} \theta_i(t) - \theta_j(t) = \theta_{ij}^{\mathrm{d}}$ $(\forall i \in \mathcal{L}, j \in \mathcal{N}_i)$. The proof is thus completed. □

Remark 5. Theorem 1 indicates that by properly selecting parameters k_1^{g}, k_2^{g} and k_3^{g}, the domain of attraction for Eq. is the whole state space under control input constraints. This is a main difference with the existing coordinated path following methods for fixed-wing UAVs in Ref.[11,12,27]. In these works, the globally asymptotic stability of the coordinated path following closed-loop is not theoretically guaranteed under control input constraints of fixed-wing UAVs.

Now we discuss the case of follower UAVs. Similar to Eqs. (13) and (14), the leader-following formation control law in the form of Eq. (6) is designed as:

$$v_i = v_l + \frac{k_1^{\mathrm{f}} \tilde{x}_i}{\sqrt{\tilde{x}_i^2 + \tilde{y}_i^2 + \delta}} \tag{31}$$

$$\omega_i = \omega_l + \frac{k_2^{\mathrm{f}} v_l \left(-\tilde{x}_i \sin\frac{\tilde{\psi}_i}{2} + \tilde{y}_i \cos\frac{\tilde{\psi}_i}{2}\right)}{\sqrt{\tilde{x}_i^2 + \tilde{y}_i^2 + \delta}} + k_3^{\mathrm{f}} \sin\frac{\tilde{\psi}_i}{2} \tag{32}$$

where k_1^{f}, k_2^{f} and k_3^{f} are positive constants satisfying

$$\begin{cases} k_1^{\mathrm{f}} \leqslant \min(v_{\max} - v_l^+, v_l^- - v_{\min}) \\ \omega_l^+ + k_2^{\mathrm{f}} v_l^+ + k_3^{\mathrm{f}} \leqslant \omega_{\max} \end{cases} \tag{33}$$

with $v_{\min} < v_l^- < v_l^+ < v_{\max}$, $\omega_l^+ < \omega_{\max}$, and $\tilde{x}_i$, $\tilde{y}_i$, $\tilde{\psi}_i$ in Eqs. (31) and (32) are defined as:

$$\begin{bmatrix} \tilde{x}_i \\ \tilde{y}_i \\ \tilde{\psi}_i \end{bmatrix} = \begin{bmatrix} \cos\psi_i & \sin\psi_i & 0 \\ -\sin\psi_i & \cos\psi_i & 0 \\ 0 & 0 & 1 \end{bmatrix} \begin{bmatrix} x_l - x_i + d_i^x \\ y_l - y_i + d_i^y \\ \psi_l - \psi_i \end{bmatrix} \tag{34}$$

The stability of the follower control closed-loop is summarized as the following theorem.

Theorem 2. Follower control stability. Consider a swarm of UAVs with the group-based hierarchical architecture established in Section 2.2. The group leaders are controlled by Eqs. (17)–(18) and (26)–(27), and the follower UAVs are controlled by Eqs. (31)–(32). For each follower $i \in \mathcal{F}_l$, Problem 3 can be solved if $v_l \in [v_l^-, v_l^+] \subset [v_{\min}, v_{\max}]$, $\omega_l \in [-\omega_l^+, \omega_l^+] \subset [-\omega_{\max}, \omega_{\max}]$, and inequalities in Eq. (33) hold.

Proof. Firstly, consider the case where l is a group leader, and thus i is in the first follower layer. It follows from Theorem 1 that $\tilde{x}_l$, $\tilde{y}_l$, $\dot{\tilde{x}}_l$, $\dot{\tilde{y}}_l$, $\dot{\tilde{\psi}}_l$ are all bounded with controllers Eqs. (17)–(18) and Eqs. (26)–(27). Besides, $\ddot{s}_l$ exists and is bounded under Assumption 1 and the updating law Eqs. (17)–(18). Therefore, $\dot{v}_l$ exists and is bounded. By using Lemma 1, we conclude that $\lim_{t\to\infty} \tilde{x}_i(t) = 0$, $\lim_{t\to\infty} \tilde{y}_i(t) = 0$, $\lim_{t\to\infty} \tilde{\psi}_i(t) = 0$. With the coordinate transformation Eq. (34), it yields $\lim_{t\to\infty} x_i(t) - x_0(t) = d_i^x$, $\lim_{t\to\infty} y_i(t) - y_0(t) = d_i^y$, $\lim_{t\to\infty} \psi_i(t) - \psi_0(t) = 0$. Moreover, it follows from similar analysis with Lemma 1 that $\tilde{x}_i$, $\tilde{y}_i$, $\dot{\tilde{x}}_i$, $\dot{\tilde{y}}_i$, $\dot{\tilde{\psi}}_i$ are all bounded with controllers (31)–(32), and thus $\dot{v}_i$ exists and is bounded.

Proceeding forward, it can be concluded that if l is in the $(r-1)$ th follower layer $(1 < r \leqslant n)$, then $\dot{v}_l$ exists and is

bounded. Similar to the above analysis, it yields $\lim_{t\to\infty} x_i(t) - x_l(t) = d_i^x$, $\lim_{t\to\infty} y_i(t) - y_l(t) = d_i^y$, $\lim_{t\to\infty} \psi_i(t) - \psi_l(t) = 0$ $(\forall i \in \mathcal{F}_l)$. □

Now we have proposed the control law to coordinate the fixed-wing UAV swarms with the group-based hierarchical architecture. Note that with the proposed approach, the feasible region of control inputs for UAVs in a higher hierarchy is always smaller than the UAVs' in a lower hierarchy. For example, the feasible region of control inputs for the group leaders is $[v_l^-, v_l^+] \times [-\omega_l^+, \omega_l^+]$, which is a subset of their followers'. If the number of layers increases, to ensure the UAVs in the $(n-1)$ th follower layer satisfy control input constraints inequality (2), the UAVs in higher hierarchies tend to have smaller feasible region of control inputs. As a result, the convergence speed for the whole system would decrease. On the other hand, if there is only one layer in the proposed architecture, i.e., each UAV is regarded as a leader with an assigned path to follow, the complexity of coordinated planning would increase. This complexity is much more vital when real-time planning is needed and communication bandwidth is quite limited. Therefore, it is preferred to have two layers, since it makes a balance between the convergence speed and the planning complexity.

4. Simulation results

In this section, numerical simulations of a swarm of ten UAVs in a coordination mission are provided to corroborate the effectiveness of the proposed group-based hierarchical formation control method. The UAVs are divided into two groups, and each group contains five UAVs. UAV 1 and UAV 6 are selected as the group leaders, and UAVs 2–5 and 7–10 are as their followers, respectively. The UAVs are required to pass through narrow passages and achieve coordinated coverage of a target area. To fulfill this mission, we plan two paths, and each path is for a group leader to follow. The paths are produced by B-splines[31] that pass through predefined waypoints shown in Table 1. Thus, the signed curvature of each path is continuous, and satisfies $|\kappa(\theta_i)| < 0.0064$.

The mission environment and the generated two paths are shown in Fig. 6. The two paths have equal path length, and the two group leaders aim to maintain the same path-length parameter when moving on their respective paths. Here the paths are parameterized with respect to the path-length parameter, i.e., $\theta_i = s_i$ $(i \in \mathcal{L})$, and thus the virtual targets' coordination objective is to achieve $\theta_1 - \theta_6 \to 0$ (i.e., $s_1 - s_6 \to 0$). Points A and B are two special points on the paths, corresponding to the 7th waypoints of the paths. Since the path-length parameters of points A and B are the same, the two group leaders are expected to arrive at these two points simultaneously. After UAV 1 and UAV 6 get to points A and B, the formation pattern of the swarm will reconfigure, such that the whole swarm can pass through the new narrow passage and cover the target area in a coordinated manner. Table 2 shows the desired relative positions of the follower UAVs with respect to their group leaders before and after the formation pattern reconfiguration.

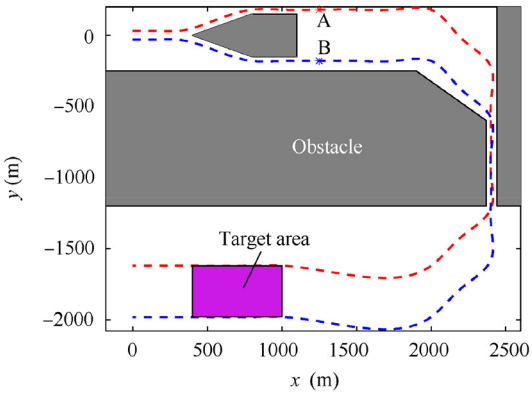

Fig. 6 Mission environment and the generated two paths for group leaders, UAV 1 and UAV 6.

The control input constraints of the UAVs are $v_{\min} = 10\text{m/s}$, $v_{\max} = 19\text{m/s}$, and $\omega_{\max} = 0.56\text{rad/s}$. Initial states of each UAV are listed in Table 3. The initial positions of the group leaders' virtual targets are set as the closest projection points of the group leaders on their respective paths, and thus $\theta_1(0) = 34.78\text{m}$, $\theta_6(0) = 15.84\text{m}$.

We first consider the architecture consisting of only two layers. Based on inequalities (28) and (33), the parameters are set as $k_1^g = k_1^f = 2$, $k_2^g = k_2^f = 0.005$, $k_3^g = k_3^f = 0.145$, $\gamma_d = 14.5$, $\gamma^+ = 0.5$, $\delta = 0.1$, and $w_{ij} = 0.3$, $\forall i,j \in L$. We use Euler method to solve The Ordinary Differential Equations (ODE) in the simulation, and the sampling time is set as 10 ms.

Table 1 Positions of waypoints in each path.

	Waypoint	# 1	# 2	# 3	# 4	# 5	# 6	# 7	# 8	# 9	# 10	# 11
Path 1	x(m)	0	150	300	550	800	1000	1250	1500	1750	2000	2200
	y(m)	30	30	30	105	180	180	180	180	180	180	−20
Path 2	x(m)	0	150	300	550	800	1000	1250	1500	1750	2000	2200
	y(m)	−30	−30	−30	−105	−180	−180	−180	−180	−180	−180	−380

	Waypoint	# 12	# 13	# 14	# 15	# 16	# 17	# 18	# 19	# 20	# 21	# 22
Path 1	x(m)	2400	2400	2400	2400	2400	2200	2000	1000	800	300	0
	y(m)	−220	−470	−720	−970	−1220	−1420	−1620	−1620	−1620	−1620	−1620
Path 2	x(m)	2400	2400	2400	2400	2400	2200	2000	1000	800	300	0
	y (m)	−580	−830	−1080	−1330	−1580	−1780	−1980	−1980	−1980	−1980	−1980

Please cite this article in press as: CHEN H et al. Formation flight of fixed-wing UAV swarms: A group-based hierarchical approach, *Chin J Aeronaut* (2020), https://doi.org/10.1016/j.cja.2020.03.006

Table 2 Desired relative positions of followers with respect to their group leaders.

	UAV i	2	3	4	5	7	8	9	10
Stage 1	d_i^x (m)	−40	−80	−120	−160	−40	−80	−120	−160
	d_i^y (m)	0	0	0	0	0	0	0	0
Stage 2	d_i^x (m)	0	0	0	0	0	0	0	0
	d_i^y (m)	−160	−120	−80	−40	40	80	120	160

Stage 1 is the stage before UAV 1 (respective UAV 6) arrive at point A (respective point B), and Stage 2 is the stage after UAV 1 (respective UAV 6) arrive at point A (respective point B).

Table 3 Initial states of each UAV.

UAV i	1	2	3	4	5	6	7	8	9	10
$x_i(0)$ (m)	34.74	–26.50	–90.12	–105.07	–144.25	15.86	6.34	–33.53	–110.31	–137.54
$y_i(0)$ (m)	57.01	26.74	38.78	42.56	45.28	–57.93	–24.88	–46.57	–14.92	–44.69
$\psi_i(0)$ (rad)	–0.08	–0.28	0.23	0.19	–0.42	–0.15	0.01	0.25	0.49	0.58

Fig. 7 presents the formation flight results of the 10-UAV swarm. The desired paths for the two group leaders are shown in dashed lines, and the trajectories of all the UAVs are shown in solid lines. The wedges indicate the positions and headings of the UAVs. In Fig. 7(a), the UAVs form two clusters, and each cluster corresponds to one group of the proposed architecture. Fig. 7(b) shows the process of UAVs merging into one common cluster and the whole swarm forming a one-line formation pattern. Fig. 7(c) shows the UAVs pass through a narrow passage in a line. The UAVs keeps this formation pattern to cover the target area in Fig. 7(d).

To further investigate the performance of the proposed method, Fig. 8 shows the errors of each UAV during the formation flight. The coordination error of group leaders' virtual targets is defined as $\tilde{\theta}_i = \sum_{j\in\mathcal{N}_i}\theta_j - \theta_i$ for UAV i, where $i \in \mathcal{L}$. Thus $\tilde{\theta}_1 = \theta_6 - \theta_1$, and $\tilde{\theta}_6 = \theta_1 - \theta_6$. Clearly, if $\tilde{\theta}_i = 0$ holds for any $i \in \mathcal{L}$, it means $\theta_i - \theta_j = 0$, $\forall i, j \in L$. It can be seen from Fig. 8 that both $\tilde{\theta}_1$ and $\tilde{\theta}_6$ converge to 0, meaning the virtual targets of the two group leaders are finally well coordinated. According to Eq. (17), we have $\dot{\theta}_i \to \gamma_d$ $(i \in \mathcal{L})$, i.e., θ_i will finally increase at a constant speed. Since both the group leader control problem and follower control problem can be regarded as a tracking problem, we show $\tilde{x}_i, \tilde{y}_i$, and $\tilde{\psi}_i$ in Fig. 8. Note that the formation reconfiguration occurs at t = 86.2 s, which results in jumps of the tracking errors. It can be seen that $\tilde{x}_i, \tilde{y}_i$, and $\tilde{\psi}_i$ all converge to zero, meaning

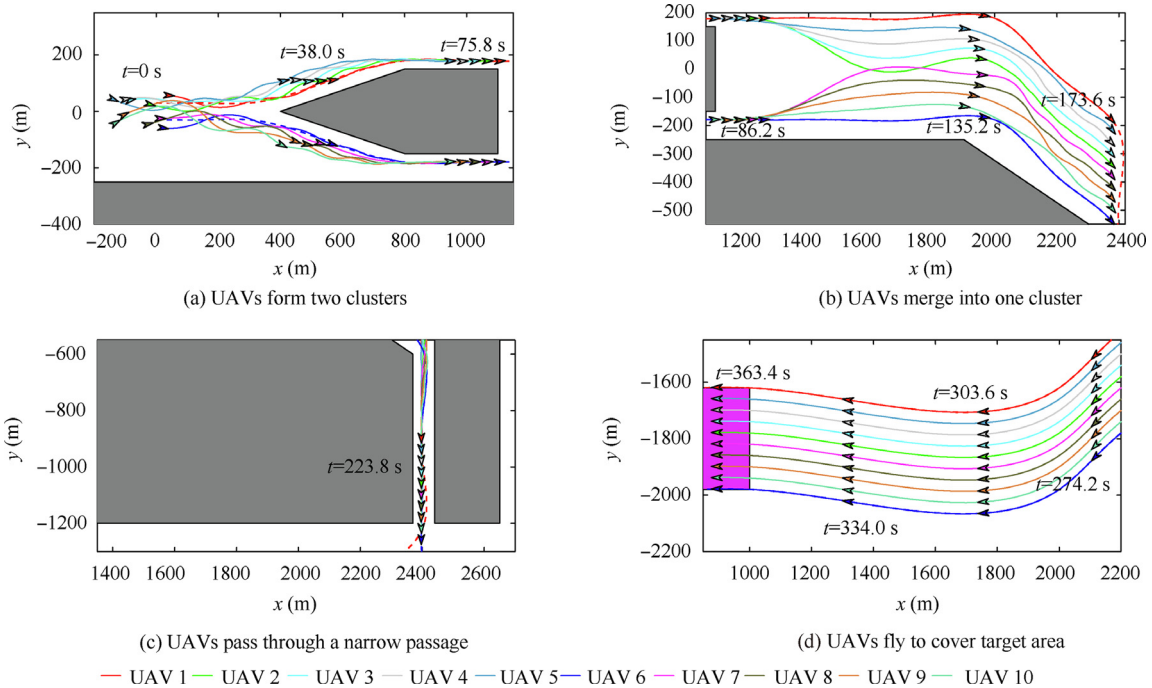

(a) UAVs form two clusters

(b) UAVs merge into one cluster

(c) UAVs pass through a narrow passage

(d) UAVs fly to cover target area

Fig. 7 Trajectories of all UAVs.

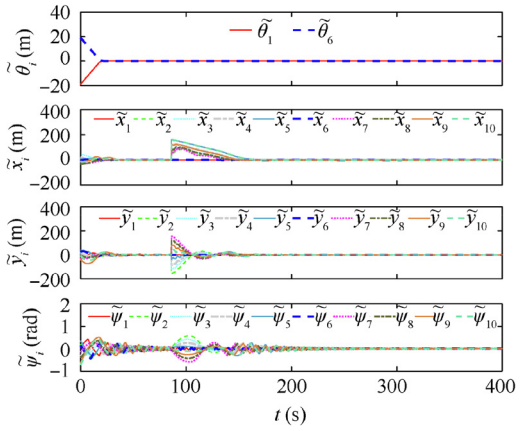

Fig. 8 Errors of each UAV during formation flight.

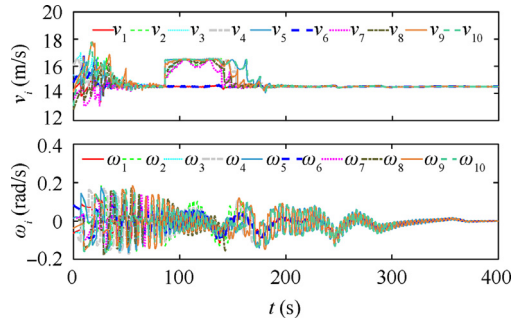

Fig. 9 Control inputs of each UAV during formation flight.

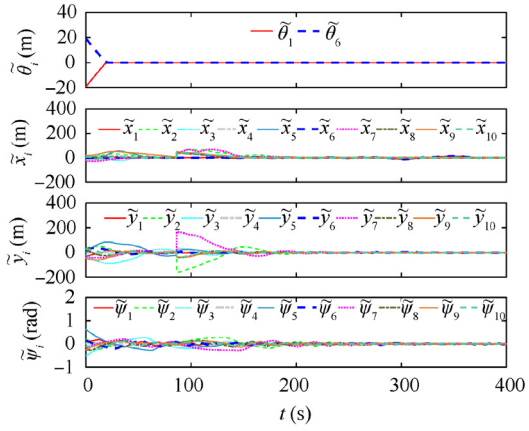

Fig. 10 Errors of each UAV in simulation with 5 layer architecture.

the control objectives in Problem 2 and Problem 3 are achieved, and all the UAVs are finally well coordinated.

Fig. 9 shows that all the UAVs' forward speeds and heading rates always satisfy the control input constraints inequality (2). Besides, all the UAVs' control inputs converge to the equal value.

In comparison, we next consider the architecture consisting of 5 layers. That is, UAVs in each group form a directed chain topology, UAV 1→UAV 2→UAV 3→UAV 4→UAV 5 in group 1, and UAV 6→UAV 7→UAV 8→UAV 9→UAV 10 in group 2. To satisfy the parameter constraints inequality (28) and inequality (33), the control parameters are set as $k_1^g = k_1^f = 0.8$, $k_2^g = k_2^f = 0.01$, $k_3^g = k_3^f = 0.076$. The mission specification and other parameters are the same with the above simulation with the architecture consisting of only two layers.

Fig. 10 shows the errors of each UAV in the simulation with the architecture consisting of 5 layers. Since the parameters for tracking become smaller due to the increase of number of layers in the architecture, it takes longer time for the tracking errors to converge to zero in Fig. 10 than in Fig. 8.

5. Conclusions

In this paper, we address the problem of formation flight of fixed-wing UAV swarms. The UAVs are organized in several distinct and non-overlapping groups, and form hierarchies in each group. There are two types of UAVs in the swarm, group leader UAVs and follower UAVs. We design coordinated path following control law for the group leader UAVs, to let these UAVs fly along their respective paths, while achieving inter-group coordination according to the mission specification. Besides, a leader-following formation control law is proposed for the follower UAVs to make these UAVs coordinate with their direct leaders. The proposed approach is distributed, scalable, and provide guarantees on formation patterns. Moreover, the globally asymptotic stability with the proposed method is guaranteed by properly selecting parameters. Results of theoretical analysis and numerical simulations indicate that the architecture with two layers is preferred, and demonstrate the effectiveness of the proposed method.

Future work includes the validation of the proposed method with actual fixed-wing UAV platforms, considering the limited-budget coordination,[45] wind disturbances, and three-dimensional formation control law.

Acknowledgements

This work was supported in part by National Natural Science Foundation of China (Nos. 61973309, 61801494 and 61702528), in part by Hunan Provincial Innovation Foundation for Postgraduate, China (No. CX2017B014).

References

1. Gupta L, Jain R, Vaszkun G. Survey of important issues in UAV communication networks. *IEEE Commun Surv Tutorials* 2016;**18**(2):1123–52.
2. Chung SJ, Paranjape A, Dames P, et al. A Survey on aerial swarm robotics. *IEEE Trans Rob* 2018;**34**(4):837–55.
3. Shakeri R, Al-Garadi MA, Badawy A, et al. Design challenges of multi-UAV systems in cyber-physical applications: A comprehensive survey and future directions. *IEEE Commun Surv Tutorials* 2019;**21**(4):3340–85.
4. Wang H, Zhao H, Zhang J, et al. Survey on unmanned aerial vehicle networks: A cyber physical system perspective Available from. *IEEE Commun Surv Tutorials* 2020;**22**(2):1027–270.
5. Keller J, Thakur D, Likhachev M, et al. Coordinated path planning for fixed-wing UAS conducting persistent surveillance missions. *IEEE Trans Autom Sci Eng* 2017;**14**(1):17–24.
6. Wang XK, Shen LC, Liu ZH, et al. Coordinated flight control of miniature fixed-wing UAV swarms: Methods and experiments. *Sci China Inf Sci* 2019;**62**(11) 212204.

7. Liu ZH, Wang XK, Shen LC, et al. Mission oriented miniature fixed-wing UAV swarms: A multi-layered and distributed architecture[Internet]. 2019 Dec [cited 2019 Dec 13]. vailable from: https://arxiv.org/abs/1912.06285.
8. Ge XH, Han QL, Zhang XM. Achieving cluster formation of multi-agent systems under aperiodic sampling and communication delays. *IEEE Trans Ind Electron* 2018;**65**(4):3417–26.
9. Zhao YY, Wang XK, Wang C, et al. Systemic design of distributed multi-UAV cooperative decision-making for multi-target tracking. *Auton Agent Multi-Agent Syst* 2019;**33**(1–2):132–58.
10. Vásárhelyi G, Virágh C, Somorjai G, et al. Optimized flocking of autonomous drones in confined environments. *Sci Robotics* 2018;**3**(20):eaat3536.
11. Xargay E, Kaminer I, Pascoal A, et al. Time-critical cooperative path following of multiple unmanned aerial vehicles over time-varying networks. *J Guidance, Control, and Dynamics* 2013;**36**(2):499–516.
12. Chen H, Cong YR, Wang XK, et al. Coordinated path following control of fixed-wing unmanned aerial vehicles. [Internet]. 2019 Aug [cited 2019 Dec 1]. https://arxiv.org/abs/1906.05453?context=eess.SP.
13. Kim H, Shim H, Back J, et al. Consensus of output-coupled linear multi-agent systems under fast switching network: Averaging approach. *Automatica* 2013;**49**(1):267–72.
14. Cao YC, Yu WW, Ren W, et al. An overview of recent progress in the study of distributed multi-agent coordination. *IEEE Trans Ind Inf* 2013;**9**(1):427–38.
15. Oh KK, Park MC, Ahn HS. A survey of multi-agent formation control. *Automatica* 2015;**53**:424–40.
16. Wang XK, Zeng ZW, Cong YR. Multi-agent distributed coordination control: Developments and directions via graph viewpoint. *Neurocomputing* 2016;**199**:204–18.
17. Zou Y, Zhou ZQ, Dong XW, et al. Distributed formation control for multiple vertical takeoff and landing UAVs with switching topologies. *IEEE/ASME Trans Mechatron* 2018;**23**(4):1750–61.
18. Kang SM, Park MC, Ahn HS. Distance-based cycle-free persistent formation: Global convergence and experimental test with a group of quadcopters. *IEEE Trans Ind Electron* 2017;**64**(1):380–9.
19. Zelazo D, Franchi A, Bülthoff HH, et al. Decentralized rigidity maintenance control with range measurements for multi-robot systems. *Int J Rob Res* 2014;**34**(1):105–28.
20. Yu YG, Li ZK, Wang XK, et al. Bearing-only circumnavigation control of the multi-agent system around a moving target. *IET Control Theory Appl* 2019;**13**(17):2747–57.
21. Kushleyev A, Mellinger D, Powers C, et al. Towards a swarm of agile micro quadrotors. *Autonomous Robots* 2013;**35**(4):287–300.
22. Wilson DB, Goktogan AH, Sukkarieh S. Vision-aided guidance and navigation for close formation flight. *J Field Rob* 2016;**33**(5):661–86.
23. Sun ZY, de Marina HG, Seyboth GS, et al. Circular formation control of multiple unicycle-type agents with nonidentical constant speeds. *IEEE Trans Control Syst Technol* 2019;**27**(1):192–205.
24. Sun GB, Zhou R, Xu K, et al. Cooperative formation control of multiple aerial vehicles based on guidance route in a complex task environment. *Chin J Aeronaut* 2020;**33**(2):701–20.
25. Chung TH, Clement MR, Day MA, et al. Live-fly, large-scale field experimentation for large numbers of fixed-wing UAVs. Proceedings of IEEE International Conference on Robotics and Automation (ICRA); 2016 May 16-21; Stockholm, Sweden. Piscataway: IEEE Press; 2016. p. 1255-62.
26. Beard RW, Ferrin J, Humpherys J. Fixed wing UAV path following in wind with input constraints. *IEEE Trans Control Syst Technol* 2014;**22**(6):2103–17.
27. Wang YZ, Wang DW, Zhu SQ. Cooperative moving path following for multiple fixed-wing unmanned aerial vehicles with speed constraints. *Automatica* 2019;**100**:82–9.
28. Yu X, Liu L, Feng G. Trajectory tracking for nonholonomic vehicles with velocity constraints. *IFAC-PapersOnLine* 2015;**48**(11):918–23.
29. Yu X, Liu L. Distributed formation control of nonholonomic vehicles subject to velocity constraints. *IEEE Trans Ind Electron* 2016;**63**(2):1289–98.
30. Wang L, Xi JX, He M, et al. Robust time-varying formation design for multi-agent systems with disturbances: Extended-state-observer method Available from. *Int J Robust Nonlinear Control* 2020;**30**(7):2796–808.
31. Zhao SL, Wang XK, Zhang DB, et al. Curved path following control for fixed-wing unmanned aerial vehicles with control constraint. *J Intell Rob Syst* 2018;**89**(1–2):107–19.
32. Yang J, Yin D, Shen LC. Reciprocal geometric conflict resolution on unmanned aerial vehicles by heading control. *J Guidance, Control, and Dynamics* 2017;**40**(10):2511–23.
33. Nagy M, Akos Z, Biro D, et al. Hierarchical group dynamics in pigeon flocks. *Nature* 2010;**464**(7290):890.
34. Shao JL, Qin JH, Bishop AN, et al. A novel analysis on the efficiency of hierarchy among leader-following systems. *Automatica* 2016;**73**:215–22.
35. Xu Y, Luo DL, Li DY, et al. Target-enclosing affine formation control of two-layer networked spacecraft with collision avoidance. *Chin J Aeronaut* 2019;**32**(12):2679–93.
36. Michael N, Kumar. V. Control of ensembles of aerial robots. *Proc IEEE* 2011;**99**(9):1587–602.
37. Cichella V, Kaminer I, Dobrokhodov V, et al. Cooperative path following of multiple multirotors over time-varying networks. *IEEE Trans Autom Sci Eng* 2015;**12**(3):945–57.
38. Rubenstein M, Cornejo A, Nagpal R. Programmable self-assembly in a thousand-robot swarm. *Science* 2014;**345**(6198):795–9.
39. Goerzen C, Kong Z, Mettler B. A survey of motion planning algorithms from the perspective of autonomous UAV guidance. *J Intell Rob Syst* 2010;**57**(1–4):65.
40. Tsourdos A, White B, Shanmugavel M. *Cooperative path planning of unmanned aerial vehicles*. Chichester, UK: John Wiley & Sons; 2011. p. 147–74.
41. Aguiar AP, Hespanha JP, Kokotović PV. Performance limitations in reference tracking and path following for nonlinear systems. *Automatica* 2008;**44**(3):598–610.
42. Chen H, Zelazo D, Wang XK, et al. Convergence analysis of signed nonlinear networks Available from:. *IEEE Trans Control Network Syst* 2020;**7**(1):189–200.
43. Khalil HK. *Nonlinear systems*. Upper Saddle River: Prentice Hall; 2002. p. 126–33.
44. Mesbahi M, Egerstedt M. *Graph theoretic methods in multiagent networks*. Princeton: Princeton University Press; 2010. p. 14–41.
45. Xi JX, Wang C, Yang XJ, et al. Limited-budget output consensus for descriptor multiagent systems with energy constraints. IEEE Transactions on Cybernetics 2020. Available from: https://ieeexplore.ieee.org/abstract/document/8967209.

Please cite this article in press as: CHEN H et al. Formation flight of fixed-wing UAV swarms: A group-based hierarchical approach, *Chin J Aeronaut* (2020), https://doi.org/10.1016/j.cja.2020.03.006